The Atomic Heat of Silicon below 100°K*

N. PEARLMAN† AND P. H. KEESOM
Department of Physics, Purdue University, West Lafayette, Indiana
(Received July 7, 1952)

The atomic heat of Si containing less than 0.01 percent P-type impurities has been measured between 1°K and 100°K. Below 5°K, the atomic heat can be represented by the sum of a cubic term with Debye $\theta=658$°K, and a linear term equal to that of a highly degenerate "hole gas" with concentration about 10^{18} cm^{-3}. This is also the hole concentration calculated from Hall constant measurements on this material. The Debye θ calculated from elastic constants is 653°K, using a simplified procedure (described in Appendix II) based on the Hopf-Lechner method. The atomic heat is in reasonable agreement with measurements of Nernst and Schwers above 20°K, and of Anderson above 60°K. Above 5°K, θ decreases to a minimum of 456°K at $T=40$°K and then rises to 580°K at $T=100$°K.

The specific heat of glyptal lacquer, which was used to secure the heater and thermometer wires to the samples, was also measured. Below 15°K, it can be represented by

$$c=2.2\times10^{-4}T^2 \text{ joules/g deg},$$

and a table is given of values above this temperature.

I. INTRODUCTION

THE atomic heat of silicon between 1°K and 100°K has been measured as part of a program of determining low temperature atomic heats in connection with irradiation studies.[1] Previous measurements, reported by Nernst and Schwers,[2] Magnus,[3] and Anderson,[4] have covered the temperature range above 20°K. Blackman and others[5] have succeeded in using the Born-von Kármán theory[6] to calculate vibration spectra in crystalline lattices. The vibration spectrum may then be used to calculate the atomic heat. Smith[7] has calculated the vibration spectrum for diamond which has the same crystal structure as Si. She has also calculated the dependence of the Debye temperature θ on absolute temperature and compared it with the observed dependence[8] in the case of diamond, down to 100°K, or about $\theta/20$. Our measurements on Si make it possible to judge if her results are applicable to the diamond lattice in general.

II. EXPERIMENT

A. Apparatus

The method used was similar to that of Nernst and Eucken.[9] The sample was suspended by threads inside a brass vacuum can. The cap of this can was soldered to a high vacuum pumping line, which had a U-section to act as a radiation trap. The electrical connections were brought out from the can through a Kovar-glass seal in its cap. Above 20°K, the sample was surrounded by a radiation shield, closed except for several small holes and having a heater wire attached. This facilitated measurements made between 20°K–50°K, and above 77°K.

Constantan heater wire (about 100 ohms per meter) was wound around the sample and attached with glyptal lacquer for heat contact. The thermometer wires were also wound on the sample and secured with glyptal. In the helium region, we used 0.05-mm phosphor-bronze wire, kindly supplied by Dr. K. W. Taconis of Leiden. In the hydrogen and nitrogen regions, we used 0.1-mm Pb wire. Above 20°K, the heater and thermometer wires were electrically insulated from the sample by cigarette paper. The increase in resistance of the sample with decreasing temperature made this unnecessary below 20°K.

B. Procedure

The rate of energy dissipation in the heater wire was determined by measuring the current passing through it and either the voltage across it or its resistance. Resistances of both heater and thermometer wires were measured by comparison with a standard 10-ohm resistor, using a Wenner potentiometer which had been certified by the National Bureau of Standards. Current and voltage were measured with instruments that had been calibrated with the standard resistor and the potentiometer. We estimate the over-all error in these measurements at about 0.3 percent.

Heating periods were begun and ended by a timing circuit which counts pulses produced photoelectrically by the pendulum of a clock. This circuit was arranged so that current could be supplied to the heater during periods which were multiples of ten seconds in length. The clock was checked against timing signals broad-

* Assisted by Signal Corps Contract.
† This article contains material from the thesis submitted by N. Pearlman to the Faculty of the Graduate School of Purdue University in partial fulfillment of the requirements for the Ph.D. degree, June, 1952.
[1] Assisted by AEC contract.
[2] W. Nernst and F. Schwers, Sitzber. preuss. Akad. Wiss., Physik-math. Kl., p. 355 (1914).
[3] A. Magnus, Ann. Physik **70**, 303 (1923).
[4] C. T. Anderson, J. Am. Chem. Soc. **52**, 2301 (1930).
[5] A bibliography is found in M. Blackman, Rept. Phys. Soc. Prog. Phys. **8**, 11 (1941). See also, e.g., E. W. Montroll, J. Chem. Phys. **10**, 218 (1942); **11**, 481 (1943); **12**, 98 (1944); **15**, 575 (1947); R. B. Leighton, Revs. Modern Phys. **20**, 165 (1948).
[6] M. Born and T. von Kármán, Physik. Z. **13**, 297 (1912); **14**, 15 (1913).
[7] H. M. J. Smith, Trans. Roy. Soc. (London) **A241**, 105 (1948).
[8] K. S. Pitzer, J. Chem. Phys. **6**, 68 (1938).
[9] A. Eucken, *Handbuch der Experimentalphysik* (Akademische Verlagsgesellschaft M.B.H., Leipzig, 1929), Vol. VIII-1.

cast by WWV, and the over-all error introduced by the timing circuit is estimated at not larger than 0.01 percent.

The thermometers were calibrated against the vapor pressures of the refrigerant liquids, using the 1939 scale for helium,[10] the NBS formula for hydrogen,[11] and the values published by Keesom and Bijl for nitrogen.[12] Above 2.2°K a correction was made to the vapor pressure above the liquid surface, to take into account the hydrostatic pressure due to the liquid above the vacuum can. When necessary, the resistance of the heater wire was also measured. The calibrations were made immediately prior to each series of heat capacity measurements. Occasionally, the calibration was checked after a run. The Pb thermometer was also compared several times with a helium gas thermometer.

It was found that the resistance-temperature curve of Pb could be approximated by a straight line above about 25°K. Below this temperature a smooth curve was drawn through the experimental calibration points. The phosphor-bronze curve was also linear below about 2°K; above this the curve could be represented by a parabola. The straight line and parabola agreed with the smooth curves drawn through the calibration points to within 0.1 percent or better. Hence, in the temperature regions where they were applicable, these expressions were used to convert resistances to temperatures and also to calculate dR/dT, which enters into the determination of ΔT, the temperature rise of the specimen resulting from heating. Between 10°K and 25°K, dR/dT was determined graphically from the Pb calibration curve.

At the conclusion of the calibration the helium gas, with which the calorimeter had been filled in order to provide heat contact between the thermometer and the bath, was pumped out and a vacuum of the order of 10^{-6} mm Hg maintained in the can. The timing circuit provided a pulse every ten seconds which was made audible by a small loudspeaker, and at every signal a galvanometer reading was taken. The galvanometer sensitivity was measured frequently, so that deflections could be converted to resistances, and hence to temperatures. The temperature drift, which was usually about 10^{-5}°K per second, was followed during a "fore-period" about 2–5 minutes long. The sample was then heated, usually for 10 or 20 seconds, producing a temperature rise of several hundredths of a degree, and thereafter the temperature drift was followed for several minutes during the "after-period." The change in temperature due to heating was determined by extrapolating the fore- and after-periods, usually to the middle of the heating period. An analysis of the heat exchange between the sample and its surroundings, including a correction for the lag of the galvanometer showed that at the lowest temperatures, the extrapolation should be carried to a point somewhat earlier than the middle of the heating period (see Appendix I). This procedure was checked by taking several points at approximately the same temperature, using different heating times and different heating currents.

[10] A table of T *versus* p, based on this scale, has been issued by the Royal Society Mond Laboratory, Cambridge, England (1949).

[11] Woolley, Scott, and Brickwedde, J. Research Natl. Bur. Standards 41, 379 (1948).

[12] W. H. Keesom and A. Bijl, Physica 4, 305 (1937); Commun. Kamerlingh Onnes Lab., Leiden, No. 245d.

C. Samples

Two samples were used, both kindly supplied by the Bell Telephone Laboratories. The first, Si I, weighed about 40 g and was stated to have an impurity concentration of about 1.5×10^{-3} percent B. Because of its small mass and the fact that its shape made it necessary to apply several tenths of a gram of glyptal to secure the heater and thermometer wires, it was impossible to measure its heat capacity accurately below 4°K. The other sample, Si II, weighed about 260 g, but its impurity concentration was not known. Its more suitable shape made it possible to use only a few mg of glyptal, and so results were obtained with this sample to below 1.5°K.

D. Measurements on Glyptal

In order to correct for the heat capacity of the glyptal, especially on the smaller sample, we measured the specific heat of glyptal from 4°K to 100°K. One set of measurements was made by adding extra glyptal to the small Si sample in several steps until a total of about 1 gram had been added. The total heat capacity was measured after each addition, and from these results the atomic heat of the Si as well as the specific heat of the glyptal could be calculated. This method gave results consistent among themselves at 4°K, and from 10 to 20°K. As an independent check, a copper disk weighing about 3 grams was coated with about 300 mg of glyptal, and the total heat capacity measured from 10 to 100°K. The heat capacity of the glyptal was about 50 percent of the total at 10°K and about 30 percent of the total at 100°K. In the overlapping temperature range, from 10 to 20°K, the two sets of results agreed to within about 15 percent.

The measured specific heat of glyptal, from which the correction was determined, could be represented below 15°K by the expression

$$c(\text{glyptal}) = 2.2\times10^{-4}\, T^2 \text{ joules/g deg.} \qquad (1)$$

Values above this temperature are given in Table I. The glyptal was air dried at room temperature after application. It is possible that different drying treatment might result in variations of polymerization which might be reflected in the specific heat. We would also like to point out that Eq. (1) is merely the simplest empirical relationship based on only a few points of not very high accuracy. Hence, while it is adequate for the required correction, any theoretical inference from its analytic form would be unwarranted.

TABLE I. Specific heat of glyptal.

T°K	c joules/g degree
20	0.11
25	0.16
30	0.20
35	0.25
40	0.29
45	0.34
50	0.38
55	0.43
60	0.49
65	0.55
70	0.62
75	0.71
80	0.79
85	0.88
90	0.97
95	1.06
100	1.15

III. EXPERIMENTAL RESULTS

As mentioned above in Sec. II-C, measurements below 4°K were made only on Si II. Above 30°K, only Si I was measured. Between 10 and 30°K both were measured, and the values agreed to within the experimental error after the heat capacity of the smaller sample had been corrected for that of the glyptal used on it. The magnitude of this correction was almost 40 percent at 10°K, about 15 percent at 20°K, and about 2 percent at 100°K on the smaller sample. The correction for glyptal on the larger sample was negligible at all temperatures.

Below 5°K, the atomic heat of Si II can be represented by the expression

$$C_v = 6.83\times10^{-6}\,T^3 + 21.0\times10^{-6}\,T \text{ joules/mol deg.} \quad (2)$$

The spread of the experimental points from this relation is shown in Fig. 1, in which C_v/T is plotted against T^2; on this plot, Eq. (2) is a straight line. The coefficients in Eq. (1) were calculated by least squares from the values of 86 experimental points taken during runs on three different days.

The values of the experimental points for temperatures from 10 to 100°K and a smooth curve through them are plotted in Fig. 2, along with the values obtained in this temperature range by Nernst and Schwers,[2] and Anderson.[4] Our results agree fairly well with these earlier measurements. A smooth curve for the Debye θ is also drawn in Fig. 2. Values taken from both curves are listed in Table II. Although the measurements give C_p, $(C_p-C_v)/C_p$ is less than 10^{-4} below 100°K,[13] so we may compare our results directly with the theoretical calculations of C_v (see Sec. IV).

The over-all random instrumental error is probably less than 1 percent and is largely independent of the temperature range. At the lowest temperatures, the influence of the heat leak, enhanced by the smallness of the heat capacity of the sample, apparently introduces random errors of several percent, as indicated by the spread of the points. There is also the possibility of systematic error of about 1 percent in the hydrogen range due to uncertainty in the glyptal correction. The over-all error in the θ-values is probably under 1 percent, particularly below 50°K, where θ depends on the cube root of the atomic heat.

IV. DISCUSSION

A. Very Low Temperature Region, $T<5$°K

1. Lattice Contribution to the Atomic Heat

The fact that the atomic heat of Si II below 5°K can be represented by the sum of a cubic and a linear term in T indicates the possibility that we have reached the true T^3 region.[14] In this case the linear term would be due to a source other than the lattice (see paragraph 2 below). Blackman's calculations lead him to expect the true T^3 region at temperatures below $\theta/50$, or at least below $\theta/100$. θ calculated from the coefficient of the cubic term in Eq. (2) is 658°K, and therefore T is less than $\theta/100$ for T less than 5°K. Blackman also proposes a criterion for the true T^3 region, namely, that $\theta(E)$, the Debye temperature calculated from low temperature elastic constants, should equal $\theta(T)$, the Debye temperature calculated from the lattice atomic heat. Values of the elastic constants of Si and their temperature coefficients, both at room temperatures, have recently been published by McSkimin and collaborators.[15] We recalculated the temperature coefficients with a more recent value of the linear expansion

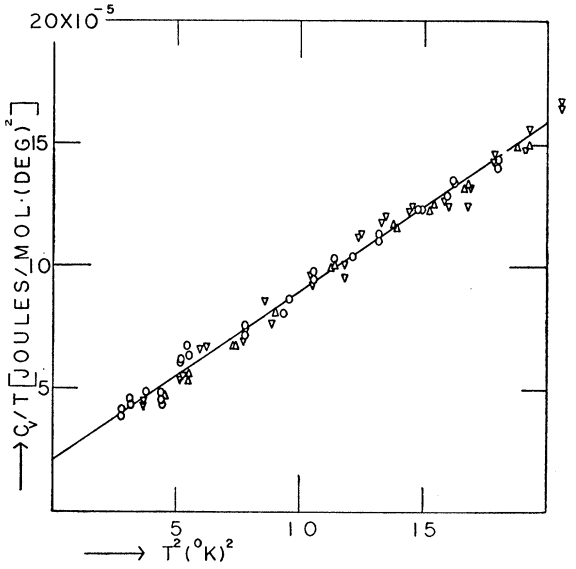

FIG. 1. C_v/T *vs* T^2 for Si. ○: 6/1/51; ▽: 5/10/51; △: 4/25/51.

[13] See, e.g., F. Seitz, *The Modern Theory of Solids* (McGraw-Hill Book Company, Inc., New York, 1940), Sec. 24.

[14] See reference 5, Sec. 3.

[15] McSkimin, Bond, Buehler, and Teal, Phys. Rev. 83, 1080 (1951).

coefficient than that apparently used there. With these data, we obtained an estimate of the elastic constants at 0°K: $c_{11}=1.689$, $c_{12}=0.6532$, $c_{44}=0.8005$, all in units of 10^{12} dynes/cm^2. The method of Hopf and Lechner,[16] modified as suggested by Durand[17] (see Appendix II), was used to calculate $\theta(E)$, for which we found 653°K. This is about 1 percent lower than $\theta(T)$. The agreement is very good in view of the accuracy of the elastic constants and the approximations involved and is further evidence that the contribution of the lattice is correctly represented by the term proportional to T^3.

2. *Nonlattice Contribution to the Atomic Heat*

The nonlattice contribution to the atomic heat can thus be represented by a term linear in temperature. Such a term is observed in the low temperature atomic heat of metals, where it is identified with the heat capacity of a strongly degenerate electron gas.[18] To see if our observed linear term might have a similar origin, the number of carriers per cm^3 n was determined by measuring the Hall constant R at and below room temperature on several small specimens cut from Si II. The resistivity ρ was also measured on these specimens. Table III presents the results, and for comparison, those of Pearson and Bardeen[19] on two of the samples in their series of measurements on B-doped Si.

The Hall constant and carrier concentration are related by[20]

$$R=r/ne. \tag{3}$$

Here e is the electronic charge, and r is a factor which varies between 1 and 2, depending on the ratio of resistivity due to impurities to total resistivity, for non-degenerate assemblies. For degenerate assemblies, r is unity. If R is given in units of cm^3/coulomb, then

$$n=r\times 6.25\times 10^{18}/R. \tag{4}$$

Two of the specimens give for n, 10^{18} cm^{-3} from room temperature down to about 10°K for specimen B and down to about 2°K for specimen C. On these specimens contacts were soldered to Rh-plated spots. Pressure probes were used on specimen A, and reliable Hall constant measurements could not be made below room temperature with this arrangement. The agreement among the resistivity values for the three specimens is as good as can be expected, considering the inhomogeneity likely to be present in an ingot weighing over 260 grams.

The heat capacity per mole due to a highly degenerate Fermi-Dirac gas is[18]

$$C_v=1.62\times 10^{-12}Vn^{\frac{1}{3}}m^*T=\gamma T \text{ joules/mole deg}, \tag{5}$$

where V is the atomic volume of the lattice, and m^* is the ratio of effective carrier mass to electron mass. Stoner[21] has shown that this equation holds for T less than 0.1 T_D, where T_D is the degeneracy temperature, given by[22]

$$T_D=4.2\times 10^{-11}n^{\frac{2}{3}}/m^* \text{ °K}. \tag{6}$$

With n equal to 10^{18} cm^{-3}, T_D is about 40°K, when m^* equals unity. This is the value found by Pearson and Bardeen[19] for the ratio of effective mass of holes to the electron mass. Thus below about 4°K, γ according to Eq. (5) is about 20×10^{-6}j/mole deg^2, which is in good agreement with the coefficient of the linear term found experimentally [see Eq. (2)], 21.0×10^{-6}j/mole deg^2.‡

The fact that the Hall constant hardly varies with T from 300°K to 2°K while T_D is only about 40°K would seem to imply that the activation energy for the impurity levels is zero and that the Fermi level is not very near the top of the filled band. The latter supposition seems reasonable, but Pearson and Bardeen[19]

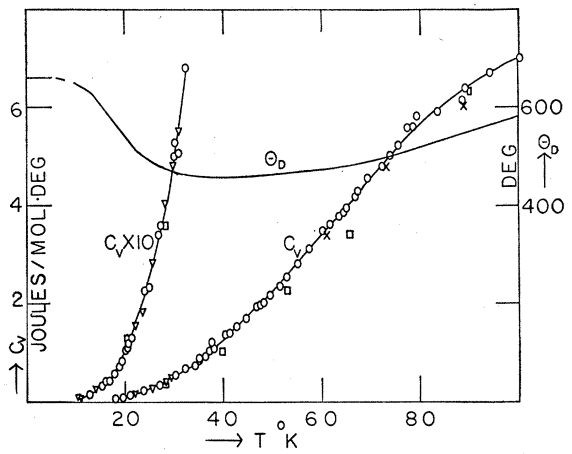

FIG. 2. C_v and θ for Si. ○: Si I; ▽: Si II; □: Nernst and Schwers; ×: Anderson.

TABLE II. Atomic heat and Debye θ of silicon.

T°K	C_v joules/mole deg	θ	T	C_v	θ
...	...	...	40	1.30	456
12	0.0130	637	45	1.78	460
13	0.0165	637	50	2.30	466
14	0.0210	623	55	2.88	472
15	0.0310	596	60	3.49	478
16	0.0400	584	65	4.08	485
17	0.0500	576	70	4.66	494
18	0.064	562	75	5.19	505
19	0.081	548	80	5.66	517
20	0.102	534	85	6.16	529
25	0.262	488	90	6.44	547
30	0.510	467	95	6.78	574
35	0.860	458	100	7.09	580

[16] L. Hopf and G. Lechner, Verhandl. deut. physik. Ges. **16**, 643 (1914).
[17] M. Durand, Phys. Rev. **50**, 449 (1944).
[18] A. Sommerfeld and H. Bethe, Handbuch der Physik (Julius Springer, Berlin, 1933), Vol. 24, part 2, pp. 347, 430.
[19] G. L. Pearson and J. Bardeen, Phys. Rev. **75**, 865 (1949).
[20] V. A. Johnson and K. Lark-Horovitz, Phys. Rev. **79**, 176 (1950); **82**, 977 (1951).
[21] E. C. Stoner, Phil. Mag. **21**, 145 (1936).
[22] V. A. Johnson and K. Lark-Horovitz, Phys. Rev. **71**, 374 (1947).

‡ *Note added in proof:*—Further electrical measurements on Si II show it to be very inhomogeneous, with both N- and P-type regions. Hence this numerical agreement may be fortuitous.

TABLE III. Electrical measurements on silicon.

Temperature region	Parameter	Our samples A	B	C	Pearson and Bardeen[a] 2	3
Room	R: cm³/coulomb	6	5	5	17	8
	ρ: ohm cm	0.14	0.14	0.10	0.14	0.06
Liquid nitrogen	R	···	5	4	200	60
	ρ	0.78	0.75	0.44	0.9	0.33
Liquid hydrogen	R (average)	···	4	4	···	···
	ρ (average)	6	3	1	···	···
Liquid helium	R (average)	···	···	5	···	···
	ρ (average)	10	130	14	···	···
Impurity atoms added to melt		?	?	?	6.7×10^{17} cm^{-3}	1.3×10^{18} cm^{-3}

[a] See reference 19.

found zero activation energy only for material having a carrier concentration at room temperature of 5×10^{18} cm^{-3} and higher. On the other hand, our resistivity values agree fairly well with those of their sample 2 both at room temperature and liquid nitrogen temperature, although only 6.7×10^{17} cm^{-3} B atoms were added to this melt. The reason for this discrepancy in the Hall constants is not clear. Further measurements are planned on a very pure single crystal of Si, in which, according to our interpretation of the present result, no linear term should be observed in the atomic heat.

B. Higher Temperature Region, $T>10°K$

It is usual to discuss the behavior in this temperature range in terms of the dependence of θ on T. Already at 12°K, the linear term in Eq. (2) is less than 2 percent of the total, so deviations from constancy of θ must be ascribed to lattice effects which are imperfectly approximated by the Debye continuum treatment.[23] Figure 3 is a plot of θ/θ_0 against T/θ_0, where θ_0 is the constant value in the true T^3 region, for Si and diamond.[24,25] For Si, θ_0 was taken as 658°K, our observed value of $\theta(T)$. For diamond, the value 1972°K was used for θ_0; this was calculated by the method of Hopf and Lechner,[16] using Smith's[7] revision of the elastic constants of diamond measured by Bhagavantam and Bhimasenachar.[26] The curve for diamond is plotted from Pitzer's measurements[8] and that for Si from the data of Table II. The circles in Fig. 3 are from θ-values calculated by Smith[7] from her determination of the elastic spectrum of diamond.

Both curves exhibit the feature found by Blackman and others in calculations on other lattices,[14] namely, that the true T^3 region ends before T equals $\theta/50$. Both curves show a dip in θ/θ_0, that for diamond being smaller and occurring at higher T/θ_0 than that for Si. This would seem to indicate that the detailed behavior of the atomic heat is not completely determined by the type of lattice.

[23] P. Debye, Ann. Physik **39**, 789 (1912).

[24] Hill and Parkinson (see reference 25) have given a similar plot, using θ_∞ as the normalizing factor rather than θ_0. 0_∞ is defined in terms of the approach of C_v to the classical value $3R$, at high temperatures.

[25] R. W. Hill and D. H. Parkinson, Phil. Mag. **43**, 309 (1952).

[26] S. Bhagavantam and J. Bhimasenachar, Proc. Roy. Soc. (London) **A187**, 381 (1946).

Katz[27] has recently shown that curves of this type may be used to derive information about the shape of the elastic spectrum. He introduces parameters q and δ_m. If the minimum in θ is θ_m and occurs at T_m, then q is given by

$$q=5T_m/\theta_0, \tag{7}$$

and δ_m is given by

$$\delta_m=(\theta_m/\theta_0)-1. \tag{8}$$

For q greater than 0.5, the spectrum is insensitive to changes in θ, so little information can be derived from q and δ_m. For q less than 0.5, a dip in θ/θ_0 corresponds to a peak in the spectrum centered about ν_p, with the weight β relative to the total area of the spectrum, where ν_p is given by

$$\nu_p=q\nu_M, \tag{9}$$

where ν_M is the maximum frequency, and β is given by

$$\beta=-11\delta_m q^3. \tag{10}$$

For the diamond curve, q is 0.5 and δ_m is -0.08, so β is 0.1. Smith[7] finds that q is 0.53 from her calculated spectrum, but the area of the peak appears to be rather larger than 10 percent of the total. These comparisons are only qualitative, since q is so large. For Si, q is 0.3, and δ_m is -0.31; β is again about 0.1. Since ν_M is proportional to θ, this would imply that ν_p for Si is about 0.2 times ν_p for diamond. These conclusions would provide a rough check on calculations of the spectrum for Si, since they apply at the low frequency end, where the accuracy of calculated spectra is poorest.

We would like to express our appreciation of the support and encouragement of Dr. K. Lark-Horovitz, who suggested the problem and provided valuable guidance in its execution. We have also benefited from stimulating discussions with Dr. H. Y. Fan. We would also like to thank Dr. D. Finlayson for performing some of the electrical measurements, L. W. Aukerman for constructing the timing circuit, and L. Babb and V. Bolyard for technical assistance.

APPENDIX I

At very low temperatures, the heat capacity of the sample is so small that it is comparable to the heat leak during one experimental point. When this is the case, the temperature during the after-period decays exponentially to that of the bath at such a rapid rate

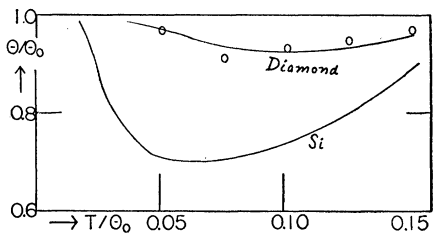

FIG. 3. θ/θ_0 *vs* T/θ_0 for diamond and Si. Curves are from atomic heat measurements; circles are Smith's calculated points for diamond.

[27] E. Katz, J. Chem. Phys. **19**, 488 (1951).

that extrapolation to the middle of the heating period no longer gives the true temperature rise. This problem has been treated by Keesom and Kok,[28] who assume that the temperature-recording instrument responds immediately to changes in T.[29-31] This implies that the maximum temperature will occur at the end of the heating-period, whereas we noticed that our galvanometer reached a maximum deflection at a time somewhat later than this whenever the final temperature of the sample was above that of the bath. Other evidence indicates that this lag is much longer than the thermal relaxation time of the specimen, so we assume that it is due to the momentum of the galvanometer and extend the treatment of Keesom and Kok[28] to take this effect into account. They derive the equations

$$T_h-T_f=(L/k)(1-e^{-kt/C}), \tag{11}$$

$$T_a-T_f=(L/k)(e^{kt_1/c}-1)e^{-kt/C}, \tag{12}$$

for the heating- and after-periods, respectively. The subscripts f, h, a refer to the fore-, heating-, and after-periods, respectively. T is absolute temperature, L the heat input per second during the heating period, and k the rate of heat loss to the surroundings per degree temperature difference per second. C is the heat capacity of the sample, t is time in seconds, $t=0$ corresponding to the beginning of the heating period, and $t=t_1$ to the end. We simplified this equation by assuming $T_f=0$, throughout the fore-period.

The differential equation for the deflection of a critically damped galvanometer which is recording the temperature of a resistance thermometer may be written as

$$(\tau/2\pi)^2\ddot{\alpha}+2(\tau/2\pi)\dot{\alpha}+\alpha=T, \tag{13}$$

where α is the galvanometer deflection and τ is the period of the galvanometer with no damping. This equation holds if T (measured here in arbitrary units) varies linearly with the current through the galvanometer, a condition which is very nearly satisfied in our measurements, since we operate in such small temperature intervals during each experimental point that the galvanometer sensitivity and dR/dT of the thermometer are essentially constant. The solution of Eq. (13) with T given by Eqs. (11) and (12) can be put in the form

$$\alpha=A_1e^{-2\pi t/\tau}+A_2te^{-2\pi t/\tau}+A_3. \tag{14}$$

Imposing the boundary conditions

$$t=0, \quad \alpha_h=0=\dot{\alpha}_h, \tag{15a}$$

$$t=t_1, \quad \alpha_a=\alpha_h; \quad \dot{\alpha}_a=\dot{\alpha}_h, \tag{15b}$$

for the beginning and end of the heating period, and

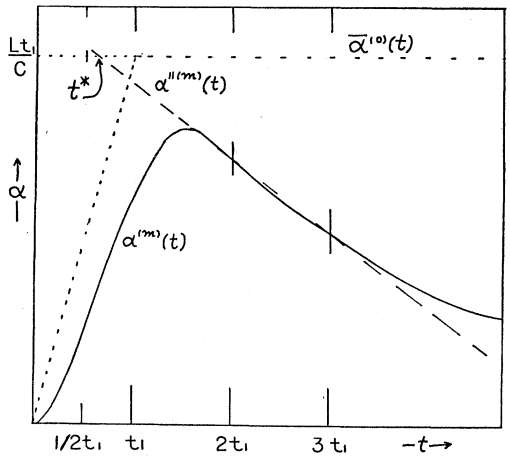

FIG. 4. Galvanometer deflection $\alpha^{(m)}(t)$ during and after heating period, illustrating extrapolation back to t^* to find true temperature rise Lt_1/C.

introducing $m=k/c$, the constants become

$$A_{1h}=(L/k)\left[\frac{4\pi^2}{(2\pi-m\tau)^2}-1\right], \tag{16a}$$

$$A_{2h}=(L/k)\left[\frac{4\pi^2}{\tau(2\pi-m\tau)}-\frac{2\pi}{\tau}\right], \tag{16b}$$

$$A_{3h}=(L/k)\left[1-\frac{4\pi^2}{(2\pi-m\tau)^2}e^{-mt}\right], \tag{16c}$$

$$A_{1a}=A_{1h}+e^{2\pi t_1/\tau}(L/k)\left[1-\frac{2\pi t_1}{\tau}-\frac{4\pi^2}{(2\pi-m\tau)^2}\times\left\{1-\frac{2\pi}{\tau}\left(1+\frac{m\tau}{2\pi}\right)t_1\right\}\right], \tag{16d}$$

$$A_{2a}=A_{2h}+e^{2\pi t_1/\tau}\times\frac{2\pi}{\tau}(L/k)\left[1-\frac{4\pi^2}{(2\pi-m\tau)^2}\left(1+\frac{m\tau}{2\pi}\right)\right], \tag{16e}$$

$$A_{3a}=\frac{4\pi^2}{(2\pi-m\tau)^2}(L/k)(e^{mt_1}-1)e^{-mt}. \tag{16f}$$

Then for the ideal case with no heat leak ($m=0$) and no lag in the galvanometer ($\tau=0$), we find the ideal temperature rise α_{id}:

$$\bar{\alpha}^{(0)}(t_1)=Lt_1/C=\alpha_{id}, \tag{17}$$

where the superscript on α indicates the value of m and the bar indicates that τ equals zero. To find α_{id} from the heating curve observed in an actual experiment, Keesom and Kok[28] extrapolate the tangent to the after-period at t_1 back to a time t^* such that

$$\alpha'^{(m)}(t^*)=Lt_1/C=\alpha_{id}, \tag{18}$$

where $\alpha'^{(m)}$ is the equation of the tangent. They find

[28] W. H. Keesom and J. A. Kok, Proc. Koninkl. Nederland. Akad. Wetenschap. **35**, 294 (1932); Commun. Kamerlingh Onnes Lab., Leiden, No. 219c.

[29] Aston and Szasz (see reference 30) and Keesom and Kurrelmeyer (see reference 31) have given generalized treatments while retaining this assumption.

[30] J. G. Aston and G. J. Szasz, J. Chem. Phys. **15**, 560 (1947).

[31] W. H. Keesom and B. Kurrelmeyer, Commun. Kamerlingh Onnes Lab., Leiden, No. 257a (1939).

TABLE IV. t^* as a function of m.

m sec^{-1}	$\alpha^{(m)}(20)$	$\alpha^{(m)}(30)$	t^* sec	$[\alpha^{(m)}(20)-\alpha^{(m)}(30)]/\alpha^{(m)}(20)$
0.001	9.8693	9.7715	6.636	0.00991
0.01	8.7840	7.9494	5.342	0.09505
0.015	8.2366	7.0906	4.613	0.1391
0.033	6.5272	4.6766	1.234	0.2816

t^* by a graphical method; we use an analytical procedure instead. We find $\alpha^{(m)}(2t_1)$ and $\alpha^{(m)}(3t_1)$ from the after-period curve, and extrapolate backwards the line between them. Calling this line $\alpha''^{(m)}$, we then have

$$\alpha''^{(m)}(t^*)=Lt_1/C=\alpha_{id} \tag{19}$$

as our equation for t^* (see Fig. 4).

To illustrate this method, we indicate the manner in which it was applied to our data. Since for our galvanometer $\tau=7$ sec, we approximated $2\pi/\tau$ by unity. We have $t_1=10$ sec; and setting $L=C$, which involves no loss in generality, we have $\alpha_{id}=10$. Inserting these values in Eqs. (16), we have

$$A_{1a}=\frac{2-m}{(1-m)^2}+e^{10}\frac{(28-9m)}{(1-m)^2}, \tag{20a}$$

$$A_{2a}=\frac{1}{1-m}+e^{10}\frac{m-3}{(1-m)^2}, \tag{20b}$$

$$A_{3a}=\frac{1}{m(1-m)^2}(e^{10m}-1)e^{-mt}. \tag{20c}$$

Equation (20c), which is the third term of our result [see Eq. (14)], differs from Eq. (12) due to Keesom and Kok only by the factor $(1-m)^{-2}$. Since we now have an analytical expression for $\alpha''^{(m)}$ in the form of a transcendental equation in t^* and m, we can find t^* for any choice of m. Values of t^* found in this way are tabulated as a function of m in Table IV. The last column in the Table IV relates m to the observed points in the after-period, and so enables one to judge where to enter the table. For $m>0.033$ the extrapolation will be very uncertain due to the large slope of $\alpha''^{(m)}$. It should be pointed out that while Keesom and Kok[28] find that t^* is never greater than $t_1/2$, we find larger values of t^* for $m=0.01$ and $m=0.001$. For such small values of m, however, the difference between $\alpha''^{(m)}(t^*)$ and $\alpha''^{(m)}(t_1/2)$ will only be of the order of 0.1 percent or less, so the extrapolation can be made to $t_1/2$.

TABLE V. Calculated data.

i, j	$j\xi$	$j\xi+C$	$f(j\xi)$	$1/120\xi^i$	a_i	λ_i	$a_i(H-L)$
0	0.0	0.413	3.767	0.00833	3.767	3.000	3.771
1	0.2	0.613	2.085	0.04167	−12.702	1.000	−12.794
2	0.4	0.813	1.634	0.2083	27.983	0.743	28.354
3	0.6	1.013	0.982	1.042	−37.845	0.625	−38.473
4	0.8	1.213	0.749	5.208	27.498	0.539	28.046
5	1.0	1.413	0.595	26.04	−8.124	0.470	−8.307

APPENDIX II

The labor involved in using the Hopf-Lechner method[16] to find $\bar{v}$, defined by

$$\frac{1}{\bar{v}^3}=\frac{1}{4\pi}\cdot\frac{1}{3}\int\sum_{k=1}^{3}\frac{1}{v_k^3}d\Omega, \tag{21}$$

where the v_k are the three sound velocities in each direction, is greatly reduced by the scheme outlined below. In the notation of Born and von Kármán[32] for a cubic crystal,

$$C=c_{44}/C'',\quad C'=(c_{12}+c_{44})/C'',\quad C''=c_{11}-c_{44}, \tag{22}$$

where c_{11}, c_{12}, and c_{44} are the three independent elastic constants for a cubic crystal in Voigt's notation.[33] When $c_{11}<c_{12}+2c_{44}$ (this corresponds to $C'>1$), we define

$$5\xi=\tfrac{1}{3}(1+2C'). \tag{23}$$

This corresponds to the generalization suggested by Durand[17] of the original treatment of Hopf and Lechner. They considered only the case in which $c_{11}>c_{12}+2c_{44}$ ($C'<1$), in which case Eq. (23) must be replaced by

$$5\xi=1. \tag{24}$$

Then introducing

$$f(j\xi)=(j\xi+C)^{-\frac{3}{2}},\quad j=0, 1, \cdots 5, \tag{25}$$

the coefficients a_i are defined by

$$a_i=\frac{1}{120\xi^i}\sum_{j=0}^{5}\alpha_{ij}f(j\xi), \tag{26}$$

where the coefficients α_{ij} are given by the matrix

$$\begin{Vmatrix} 120 & 0 & 0 & 0 & 0 & 0 \\ -274 & 600 & -600 & 400 & -150 & 24 \\ 225 & -770 & 1070 & -780 & 305 & -50 \\ -85 & 355 & -590 & 490 & -205 & 35 \\ 15 & -70 & 130 & -120 & 55 & -10 \\ -1 & 5 & -10 & 10 & -5 & 1 \end{Vmatrix}=(\alpha_{ij}). \tag{27}$$

Introducing the constants

$$\beta_1=1-C'^2,\quad \beta_0=1-3C'^2+2C'^3, \tag{28}$$

we define

$$\begin{aligned} &\lambda_0=3;\quad \lambda_1=1,\\ &\lambda_2=\left(1-\frac{2}{5}\beta_1\right),\\ &\lambda_3=\left(1-\frac{3}{5}\beta_1+\frac{1}{35}\beta_0\right),\\ &\lambda_4=\left(1-\frac{4}{5}\beta_1+\frac{4}{105}\beta_0+\frac{2}{21}\beta_1^2\right),\\ &\lambda_5=\left(1-\beta_1+\frac{1}{21}\beta_0+\frac{5}{21}\beta_1^2-\frac{1}{77}\beta_0\beta_1\right), \end{aligned} \tag{29}$$

[32] M. Born and T. von Kármán, Physik. Z. 14, 15 (1914).
[33] W. Voigt, *Lehrbuch der Kristallphysik* (B. G. Teubner, Leipzig, 1928).

and write

$$I_{HL}=\frac{1}{3}\sum_{i=0}^{5}\lambda_i a_i. \quad (30)$$

The final result is then

$$\bar{v}=(I_{HL})^{-\frac{1}{3}}(C''/\rho)^{\frac{1}{2}}\ \text{cm/sec} \quad (31)$$

and

$$\theta(E)=2.514\times10^{-3}\bar{v}/(V)^{\frac{1}{3}}, \quad (32)$$

where ρ is the density of the crystal and V the atomic volume.

It should be pointed out that Eq. (32) holds only when the Debye treatment gives an adequate approximation to the atomic heat, that is, in the true T^3 region. Thus the elastic constants should be those at 0°K. It can be seen from Eqs. (30) and (31), however, that $\theta(E)$ is not extremely sensitive to variation of the c_{ij}. To illustrate the method, we apply it to the data given by Hopf and Lechner for FeS_2: $\rho=5.03$ g/cm^3, $C=0.413$, $C'=0.598$, $C''=2.555\times10^{12}$ dynes/cm^2. Since $C'<1$, $\xi=0.2$. From Eq. (28), $\beta_1=0.642$, $\beta_0=0.355$. Table V lists the quantities calculated from these data. The last column gives the coefficients computed by Hopf and Lechner. From this table we calculate $I_{HL}=2.25$; and $\bar{v}=5.46\times10^5$ cm/sec. The values given by Hopf and Lechner are 2.26 and 5.43×10^5 cm/sec.

PHYSICAL REVIEW VOLUME 88, NUMBER 2 OCTOBER 15, 1952

Production of the *E*-Layer in the Oxygen Dissociation Region in the Upper Atmosphere

D. C. CHOUDHURY
Institute of Radio-Physics and Electronics, Calcutta University, Calcutta, India

(Received April 25, 1952)

Starting with the generally accepted theory that the *E*-layer is formed by ionization of O_2 in the region of its dissociation, the probable value of the absorption cross section of O_2 for this ionization is calculated by utilizing the height distribution of O_2 (in the transition region) as recently obtained by Moses and Wu. It is found that, depending upon the temperature gradient and the boundary temperature chosen for the region of dissociation, the necessary absorption cross section varies from 3×10^{-19} cm^2 to 9×10^{-18} cm^2. Hence, it follows that for the two current hypotheses of *E*-layer ionization, namely, pre-ionization by solar rays in the wavelength range 900A–1000A (Nicolet) and ionization by high energy photons emitted from the solar corona (Hoyle and Bates), the ionization cross section of O_2 should also lie within this range. For the former, the rate of ion production (as obtained by application of simple Chapman formula and assuming the sun to be radiating like a blackbody) appears to be one hundred times more than the observed rate. The discrepancy is removed if it is assumed that of the molecules excited to the pre-ionization levels by absorption, only a small fraction (one in a hundred) undergoes ionization. For the high energy photons it is found that in order to have the necessary absorption cross section, the energy should be 181 ev rather than 325 ev as obtained by Hoyle and Bates. It is suggested that both the pre-ionization process and the ionization by high energy photons are operative in producing *E*-layer ionization. The former produces the normal *E*-layer and the latter (of different frequencies) intensifies the ionization at different levels producing the fine structure of the *E*-layer as reported recently.

1. INTRODUCTION

THE most generally accepted theory of the *E*-layer is that it is formed by the ionization of molecular oxygen in the region where its concentration falls rapidly with height owing to photodissociation (Mitra,[1] Bhar,[2] and Wulf and Deming[3]). There is, however, uncertainty regarding the process of ionization and the wavelength of the active radiation. According to the earlier views, the ionization of O_2 was either at its first ionization potential (Wulf and Deming[3]) or at its second ionization potential (Bhar[2]). There have, however, been objections to both these views. For the first ionization potential (12.2 ev) the absorption cross section is so small that no ionization maximum will be formed in the region of dissociation. (Ionization at the first ionization potential of O_2 is now believed to produce the *D*-region.[4]) Again, the wavelength range of the active radiation for the second ionization potential 760–661A lies within the region of strong absorption of atomic oxygen. Hence, the active radiation will all be used up before reaching the transition level. To meet these difficulties two different hypotheses have been proposed. According to one (Hoyle and Bates[5]) emissions of very high energy photons (perhaps of about 325 ev) from the solar corona is supposed to cause the ionization. According to the other (Nicolet[6]) pre-ionization of molecular oxygen by solar radiation in the energy range 12.2 to 13.55 ev (900A to 1000A) is responsible for the ionization of O_2.

In the present note the recent theoretical determinations of the distribution of molecular oxygen in the region of dissociation, as made by Moses and Wu,[7] will be utilized to first find out what should be the value of the absorption cross section of O_2, in order that the *E*-peak may be formed at the observed height.

[1] S. K. Mitra, Nature **142**, 914 (1938).
[2] J. N. Bhar, Indian J. Phys. **12**, 363 (1938).
[3] O. R. Wulf L. S. and Deming, Terr. Mag. Atmos. Elect. **43**, 283 (1938).
[4] A. P. Mitra, J. Geophys. Research **56**, 373 (1951).
[5] F. Hoyle and D. R. Bates, Terr. Mag. Atmos. Elect. **53**, 51 (1948).
[6] M. Nicolet, Mem. Roy. Met. Inst. Belge, **19**, 124 (1945).
[7] H. E. Moses and T.-Y. Wu, Phys. Rev. **83**, 109 (1951).